Viscoelastic Shear Response and Network Structure in Polycyanurates

Qingxiu Li and Sindee L. Simon*

Department of Chemical Engineering, Texas Tech University, Lubbock, Texas 79409-3121

Received October 20, 2006; Revised Manuscript Received December 12, 2006

ABSTRACT: The shear response of polycyanurate networks with different cross-link densities, varied by changing the ratio of difunctional to monofunctional cyanate ester, is measured from shear stress relaxation and dynamic experiments. Master curves are constructed following the time−temperature superposition principle, and the temperature dependence of the shift factors is examined. The discrete relaxation time spectra are calculated from the viscoelastic responses and are found to be independent of cross-link density over the time/frequency range measured. The cross-link density, determined from the rubbery modulus, and the sol content, measured from sol extraction experiments, are modeled for the fully cured polycyanurate networks using the recursive method; a monomer cyclization reaction is assumed in the modeling based upon the chemical composition of the sol which was determined by mass spectroscopy. The effect of monomer cyclization on the conversion at gelation of dicyanate esters is discussed.

Introduction

In the 1980s, cyanate ester resins gained attention in the electronic and aerospace composite industries due to their unique properties, including high glass transition temperature, low dielectric loss, low moisture absorption, and relatively high fracture toughness.[1−34] Cyanate esters cure by a cyclotrimerization reaction to form polycyanurate networks. The gelation point of dicyanate ester/polycyanurate resins is expected to occur at a conversion of 0.5 based on Flory's mean-field theory.[35] However, a survey of the literature, summarized in Table 1, indicates that either theoretical or delayed gelation behavior can be observed. Georjon et al.,[4] Kasehagen et al.,[5] Stutz et al.,[6] and Mormann et al.[7] report that the gel point for bisphenol A dicyanate ester cured under inert gas environment (or unspecified gas environment) is consistent with the theoretical value, in agreement with an earlier result from Bauer and Bauer.[2,3] Nevertheless, a majority of studies reveal that the experimental conversion at the gel point for bisphenol A and bisphenol M dicyanate esters is larger than expected, ranging from 0.58 to 0.64.[1,8−10,12−15,36] The delayed gelation behavior has been attributed to unequal reactivity of functional groups induced by diffusion control before gelation,[11,26] intracyclization before gelation,[12,15,18,27,28,31] dimerization reactions resulting in formation of a four-membered CNCN ring,[8,10,30] and side reactions involving water.[4,5] It has been argued that the dimerization side reaction may not be the contributing factor based on X-ray crystallographic data,[37] NMR data,[29] and energy level calculations of the parent diazacyclobutadiene.[28] Wang et al. also demonstrated that the contribution from the dimer for the delayed gelation of a rigid spiro-aromatic dicyanate is not significant.[18] Furthermore, water is expected to not be the sole cause of delayed gelation because most of the studies which reveal delayed gelation were performed under inert gas environments.

As indicated by the data shown in Table 1, the gelation delay in polycyanurate thermosetting systems depends on the monomeric backbone structure and the cure reaction conditions. As already mentioned, in the studies which reveal delayed gelation, the conversion at gelation ranges from 0.58 to 0.64 for bisphenol A[8−10,12−15,36] and bisphenol M dicyanate ester monomers.[1] Delayed gelation is also found for other cyanate esters such as 4,4′-thiodiphenyl cyanate (TDPC),[12] bis(4-cyanatophenyl) ether (OXOCY),[19] dicyanato-4,4′-diphenylethane (DPEDC),[16,17] and other cyanate esters with rigid backbone structures[18] or with functional groups having lower accessibility due to the steric hindrance.[12] In addition, the extent of gelation delay for bisphenol A dicyanate solutions in nitrobenzene and ditolylmethane increases with decreasing monomer concentration.[15] On the other hand, very flexible alkyl chain structures or backbone chains with electron-withdrawing groups lead to the gel point being closer to the theoretical value.[12,20,21] On the basis of the dependence of the gel point on the backbone structure and reaction conditions of dicyanate esters, researchers proposed that intracyclization, in which two cyanate groups on the same oligomer react with a third functional group, is the main reason for the gelation delay of cyanate esters.[12,15,18,27,28,31,38] In this work, we further examine the role of intracyclization, and in particular, monomer cyclization, through study of the viscoelastic behavior of bisphenol M dicyanate ester polycyanurate networks. We note that although the viscoelastic properties of epoxy resins are well studied,[39−43] the effect of network structure on the viscoelastic behavior of polycyanurates has not been well documented.

For cross-linked polymeric systems, the storage modulus G', loss modulus G'', and relaxation modulus $G(t)$ can be described by the sum of Maxwell elements:[44]

$$G'(\omega) = G_r + [G_g - G_r]\sum_{i=1}^{n} g_i \frac{\omega^2 \tau_i^2}{1 + \omega^2 \tau_i^2} \quad (1)$$

$$G''(\omega) = [G_g - G_r]\sum_{i=1}^{n} g_i \frac{\omega \tau_i}{1 + \omega^2 \tau_i^2} \quad (2)$$

$$G(t) = G_r + [G_g - G_r]\sum_{i=1}^{n} g_i e^{-(t/\tau_i)} \quad (3)$$

where G_g is the glassy modulus, G_r is the rubbery modulus, ω is radian frequency, t is time, τ_i is the ith relaxation time, g_i is

* Corresponding author. E-mail: Sindee.Simon@ttu.edu.

10.1021/ma0624144 CCC: $37.00
Published on Web 02/15/2007

Table 1. Literature Summary for the Conversion at Gelation of Dicyanate Esters

Monomer name	Monomer structure	β_{gel}	Atmos.	Cat. or Uncat.	Ref.
BMDC	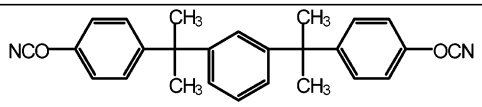	0.64	N_2	Uncat. Cat.	Simon, Gillham[1]
BADC	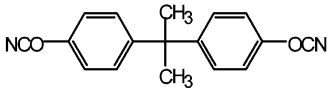	0.5	Ar	Uncat.	Bauer *et al*[2, 3]
		0.6	Air	Uncat.	Georjon *et al*[4]
		0.5	Ar		
		0.51	N_2	Cat.	Kasehagen *et al*[5]
		0.50	-	Uncat.	Stutz, Simak[6]
		0.50	-	-	Mormann *et al*[7]
		0.58-0.62	Air	Uncat.	Gupta *et al*[8]
		0.60-0.64	N_2	Cat.	Owusu *et al*[9]
		0.60	N_2	Uncat.	Grenier *et al*[10]
		0.60-0.64	-	Cat.	Deng *et al*[11]
		0.60	N_2	Uncat.	Lin *et al*[12]
		0.63	-	Uncat.	Shimp *et al*[13]
		0.58-0.62	-	Uncat. Cat.	Recalde *et al*[14]
		0.60-0.70 to 0.80-0.95	Ar	Cat. Solution	Korshak *et al*[15]
DPEDC	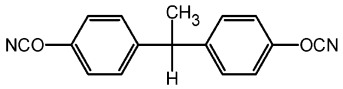	0.60	-	Cat.	Galy *et al*[16]
		0.64	N_2	Cat.	Chen *et al*[17]
TMBADC	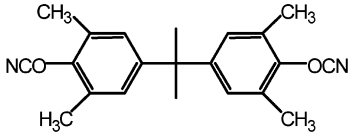	0.62	N_2	Uncat.	Lin *et al*[12]
DCSI	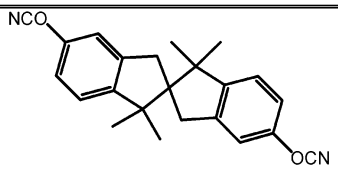	0.65	N_2	Uncat.	Wang, Hong[18]
OXOCY	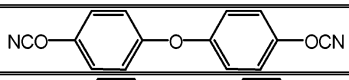	0.58-0.64	Vac.	Uncat.	Armistead, Snow[19]
TDPC	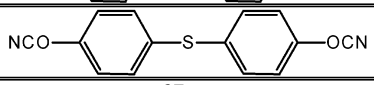	0.58	N_2	Uncat.	Lin *et al*[12]
HFBADC	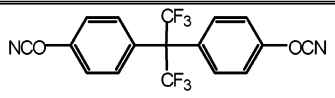	0.55	N_2	Uncat.	Lin *et al*[12]
F_6CY	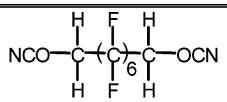	0.5	N_2	Uncat.	Snow *et al*[20]
CPS	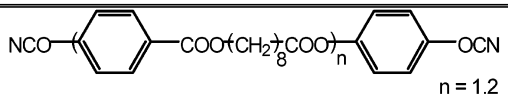	0.52	N_2	Uncat.	Lin *et al*[12]
		<0.55	-	Uncat.	Lu, Hong[21]

the weighing factor for the *i*th relaxation time, and $\sum g_i = 1$. The viscoelastic responses of cross-linked systems depend on time or frequency as indicated explicitly in eqs 1−3 and also on temperature and cross-link density since the rubbery modulus G_r and relaxation time τ_i depend on these variables. The theory of rubber elasticity describes the dependence of the rubbery modulus on temperature and cross-link density,[45] whereas the Vogel−Fulcher[46,47] equation can be used to describe the dependence of the relaxation time on temperature:[42]

$$\log a_T = \log\left(\frac{\tau_i(T,T_g)}{\tau_i(T_{ref},T_g)}\right) = C\left(\frac{1}{T-T_\infty} - \frac{1}{T_g - T_\infty}\right) \quad (4)$$

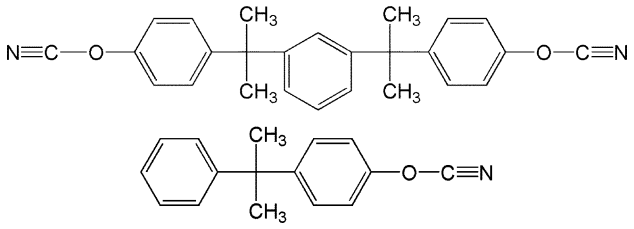

Figure 1. Chemical structure of difunctional and monofunctional cyanate esters.

where a_T is the shift factor, T is temperature, τ_i is the ith relaxation time, C is a constant, and T_{ref} is taken to be T_g. This expression can describe both WLF[48] temperature dependence, which is observed above T_g, or Arrhenius temperature dependence (when $T_\infty = 0$ K) below T_g albeit with different parameters C and T_∞. Equation 4 describes the effect of temperature on the relaxation time, but it can also be used to describe the effect of cross-link density or conversion on relaxation time since T_g is a function of these variables. Time−temperature superposition is valid if the temperature dependence of the shift factors follows eq 4. The time−cross-link density superposition principle is valid if the constant C does not vary with T_g or cross-link density, which infers that the viscoelastic response shifts to longer times with increasing cross-link density without a change in the shape of the relaxation spectrum. For the viscoelastic properties of cross-linked systems, the validity of these two principles has been demonstrated[39−41,43,49−52] or assumed, as in the modeling of the evolution of viscoelastic properties during cure.[42] However, there is evidence that time−cross-link density superposition does not hold for the long-time response. For example, Plazek's data on a series of epoxy resins show that the temperature dependence of shift factors below T_g depends on cross-link density.[40] The retardation spectrum $L(\lambda)$ and/or the relaxation spectrum $H(\tau)$ are also found to depend on cross-link density at long times for both rubber and epoxy networks.[40,41,50,51]

In the work presented here, we focus on the shear viscoelastic behavior and structure of polycyanurate networks as a function of cross-link density. The validity of time−temperature superposition and time−cross-link density superposition principles will be examined. The importance of incorporating intracyclization, and in particular monomer cyclization, in the reaction model in order to predict the experimental cross-link density, sol content, and sol structure, the latter of which is obtained by mass spectroscopy, will be discussed. The paper is organized as follows. We first present the experimental and modeling methodologies, followed by the results of the work. We then discuss the implications of the results with respect to the cause of the delayed gelation in bisphenol M, bisphenol A, and other dicyanate esters with similar structure. We end with the conclusions and an Appendix detailing the recursive calculations.

Experimental Methodology

Materials. Four fully cured cyanate ester/polycyanurate thermosetting materials having different cross-link densities were studied. One formulation consisted of difunctional cyanate ester, 4,4′-(1,3-phenylenediisopropylidene) diphenylcyanate, also referred as bisphenol M dicyanate ester or BMDC (Huntsman Advanced Materials Americas Inc.). The other three formulations were mixtures of the difunctional BMDC cyanate ester with monofunctional cyanate ester, 4-cumylphenol cyanate ester (Oakwood Products, Inc.). The molecular structures of difunctional and monofunctional cyanate esters are shown in Figure 1. The molecular weights of the difunctional and monofunctional monomers are 396 and 237 g/mol, respectively. The density for the difunctional monomer is 1.14 g/cm^3 at 25 °C; the density for the monofunctional monomer is not available. The mole fraction of cyanate groups that are monofunctional in the four formulations ranges from 0.0 to 0.3, which corresponds to 0 to 33 wt % of monofunctional cyanate ester (relative to the weight of all cyanate esters). All formulations included 2 parts by weight catalyst (ESR 273, Rhone-Poulenc High Performance Resins) per 100 parts by weight resin, and the catalyst comprises 8.5 wt % copper naphthenate in 91.5% nonylphenol.[1] The molar ratio of nonylphenol to the cyanate group varies slightly as the concentration of monofunctional cyanate ester in the formulation changes, from 0.0165 for the neat bisphenol M dicyanate ester to 0.0174 for the formulation with 0.3 mole fraction of monofunctional cyanate ester. All chemicals were used with no further purification.

Before mixing, the bisphenol M dicyanate was heated at 100 °C for 3 min to remove any crystallites formed during the storage in a freezer at around −10 °C and allowed to cool to room temperature. Formulations were mechanically stirred for 30 min at room temperature. Prior to cure, the mixtures were degassed under vacuum. Mixtures were cured in glass tubes whose inner surfaces were coated with thin layers of silicon oil to prevent sample cracking during the curing and cooling process. The formulations were cured at 180 °C for 18 h and were allowed to cool to room temperature overnight in the oven. Fourier transform infrared spectroscopy (FTIR) confirms that all of the networks are fully cured in agreement with expectations based on previous study of the cure kinetics of bisphenol M dicyanate ester.[1] The limiting fictive temperatures (T_f') of the uncured materials are −21, −24, −27, and −29 °C for mole fractions of the monofunctional monomer of 0.0, 0.1, 0.2, and 0.3, respectively, as measured by DSC on heating at 10 K/min after cooling at 10 K/min; the limiting fictive temperatures of the fully cured polycyanurate networks for the same mole fractions are 176, 149, 127, and 110 °C, respectively, again measured by DSC on heating at 10 K/min after cooling at 10 K/min. The limiting fictive temperature (T_f') obtained on heating after cooling at a given rate approximates the glass transition temperature (T_g) measured on cooling at the same specified rate;[53,54] hence, we refer to T_f' as T_g in the remainder of this paper. We note that T_f' (or T_g) of the fully cured bisphenol M dicyanate ester/polycyanurate material having no monofunctional monomer is lower than that of many commercial polycyanurates due to the monomer's higher molecular weight which leads to a lower cross-link density in the network.

Stress Relaxation and Dynamic Measurements. Shear stress relaxation and dynamic measurements were performed on an Advanced Rheometric Expansion System (ARES, Rheometric Scientific) with a 2K FRTN1 transducer. The samples, approximately 6.35 mm in diameter and 40 mm in length, were used with cylindrical sample fixtures. The sample length between the fixtures was around 25 mm as read by the instrument to a precision of ±0.001 mm. The testing temperatures ranged from $T_g - 20$ °C to $T_g + 20$ °C in 5 °C intervals for all the samples except the polycyanurate with 0.3 mole fraction of monofunctional cyanate ester, for which the testing temperatures ranged from $T_g - 10$ °C to $T_g + 30$ °C because the sample was too weak to be tested below $T_g - 10$ °C. The instrument temperature accuracy is ±0.2 °C with nitrogen as the convection gas. Before testing, the sample was held at $T_g + 10$ °C without any applied load for 30 min to erase the previous history, and then the sample was held at the testing temperature for 60 min prior to applying the strain for testing temperatures lower than $T_g + 10$ °C. When the testing temperatures were at $T_g + 10$ °C or higher, the sample was held at the testing temperature for 30 min before strain application. The stress relaxation measurements were performed for 6 min for testing temperatures lower than $T_g + 10$ °C, in accordance with Struik's protocol,[55] which allows measurements to be performed for 10% of the holding time in order to minimize the influence of physical aging during the testing. Following the stress relaxation experiments, dynamic experiments were performed at frequencies ranging from 1 to 30 rad/s; this limited range of frequencies was used to minimize the time to make the dynamic measurements. The dynamic measurements were performed for 2.3 min, which resulted in a total

measuring time of 8.3 min (13.8% of the holding time). The initial strain was set to 0.02% in the glassy region and 2% or lower in the rubbery region to ensure a linear response. The calculated instrument compliance for our results is 5% or lower;[56] therefore, no data correction was performed for the instrument compliance.

Sol Extraction Experiments. Sol extraction experiments were carried out to determine the sol content of the cured polycyanurate networks. Samples of about 100 mg were placed in extraction thimbles, which were immersed in tetrahydrofuran in a vial for 2 weeks. Following the extraction, the gels were exposed to vacuum at around their glass transition temperature for up to 2 weeks until a constant weight was achieved. The sol content was determined on the basis of weight change before and after extraction. Fourier transform infrared spectroscopy and mass spectroscopy were performed only on the sol extracted from the formulation with 0.3 mole fraction of monofunctional cyanate ester because the volume of the sol extracted from the other formulations was insufficient.

Fourier Transform Infrared Spectroscopy (FTIR). The chemical structures of the monomers, polycyanurate networks, and the sol from the formulation with 0.3 mole fraction of monofunctional cyanate ester were studied using a Thermo Nicolet Nexus 470 Fourier transform infrared spectrometer (FTIR). The monomer spectra were collected with the sample placed between two polished NaCl salt plates. Care was taken to prevent the formation of air bubbles in the sample between the salt plates. After the scans of the uncured formulations, the samples sandwiched between salt plates were immediately transferred to the oven and cured at 180 °C for 18 h. The cured samples were allowed to cool to room temperature in the oven, and FTIR spectra were collected again. The spectrum of the sol was collected after coating the sol solution in tetrahydrofuran on the salt plate and allowing the solvent to evaporate.

Mass Spectroscopy. The chemical composition of the sol extracted from the formulation with 0.3 mole fraction of monofunctional cyanate ester was analyzed using a Thermo-Electron mass spectroscope with an atmospheric pressure chemical ionization (APCI) probe running in positive mode up to 2000 *m*/*z*. The sol solution in acetone was vaporized at 350 °C and directly infused into the ionization chamber. The ionized samples were then transferred into the capillary tube at 200 °C. The mass spectrum showing the relative abundance of the ionized components as a function of mass/charge (*m*/*z*) was recorded.

Theoretical Modeling

The cross-link density and sol content of the formulations were modeled using recursive theory,[57] assuming equal reactivity of all functional groups. The effects of intracyclization, and in particular monomer cyclization, were incorporated by assigning a probability K_{intra} to the monomer cyclization reaction of two cyanate groups on the same monomer. K_{intra} is assumed to be independent of formulation. The probability of monomer cyclization was determined upon fitting the experimental cross-link density and sol content data to the theory, and a value of 0.14 was obtained. This value predicts a conversion at gelation of 0.63 for neat BMDC (without added monofunctional monomer), consistent with the experimental observation of 0.64.[1] Expressions for the cross-link density, the sol content, and the conversion at gelation are derived in the Appendix. Our derivations are consistent with recent work by Lin et al.;[12,31,38,58] the expression for the cross-link density differs from the earlier work by Simon and Gillham because that original derivation omitted the leading conversion term.

Our approach differs from the recent work by Sarmoria and Miller detailing a methodology which incorporates intracyclization prior to gelation to form both monomeric- and larger-sized rings; their work involves Monte Carlo simulations to obtain the probability of intramolecular reaction.[59] Our methodology is, in comparison, much simpler in that only monomeric-sized rings are considered and Monte Carlo simulations are not needed. In effect, we oversimplify the problem by including only monomer cyclization, but in doing so, we gain the advantage of an analytical solution.

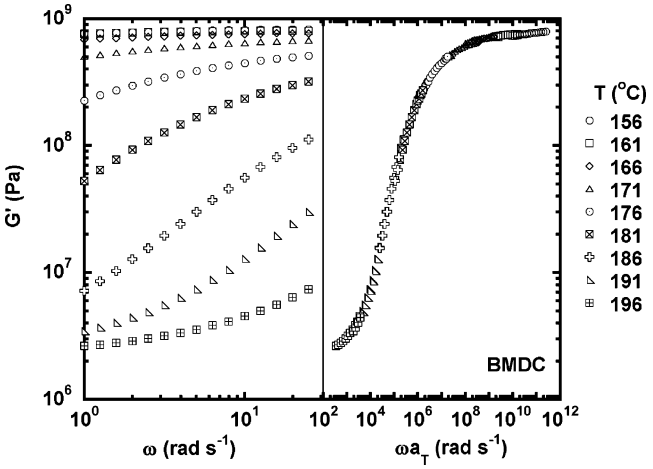

Figure 2. Storage modulus as a function of frequency for fully cured BMDC polycyanurate at temperatures ranging from 156 to 196 °C. The master curve, shifted to the right for clarity, is obtained by time−temperature superposition.

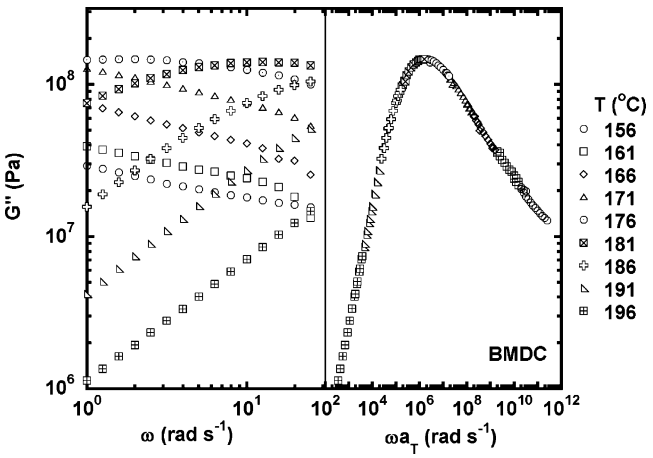

Figure 3. Loss modulus as a function of frequency for fully cured BMDC polycyanurate at temperatures ranging from 156 to 196 °C. The master curve, shifted to the right for clarity, is obtained by time−temperature superposition.

Results

Viscoelastic Properties of Polycyanurate Networks. The storage modulus and loss modulus as a function of frequency for BMDC polycyanurate without the addition of monofunctional cyanate ester at temperatures ranging from 156 to 196 °C together with their corresponding reduced curves are plotted in Figures 2 and 3. Recall that the nominal T_g for this material is ∼176 °C at a cooling rate of 10 K/min. At low testing temperatures or high frequencies, the material shows a glassy response with a modulus of ∼800 MPa. The storage modulus decreases with increasing testing temperature and with decreasing frequency. The loss modulus goes through a maximum as the testing temperature increases through the T_g region. The unreduced and reduced stress relaxation moduli are shown in Figure 4 for the same BMDC polycyanurate (without monofunctional monomer). The relaxation modulus decreases with increasing temperature and time, and at high testing temperatures and long times, the material shows a rubbery modulus at around 2.3 MPa. The successful construction of master curves for the

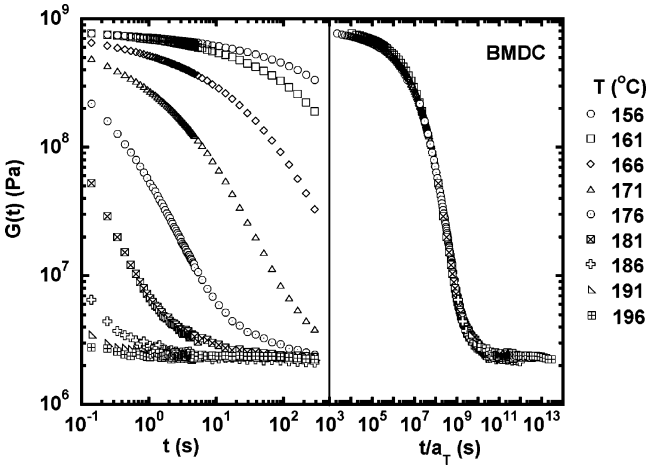

Figure 4. Relaxation modulus as a function of time for fully cured BMDC polycyanurate at temperatures ranging from 156 to 196 °C. The master curve, shifted to the right for clarity, is obtained by time−temperature superposition.

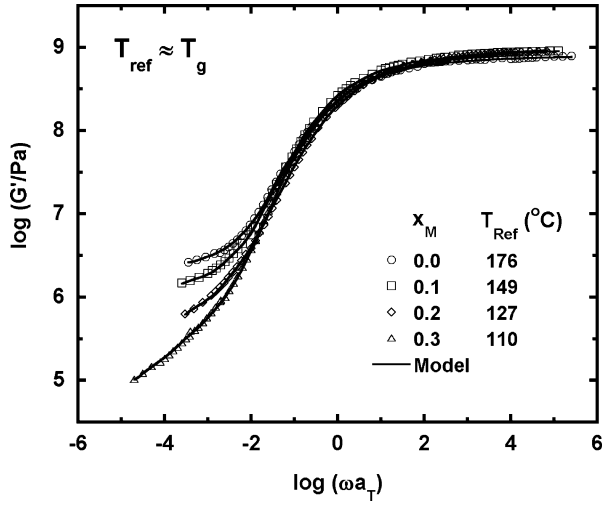

Figure 5. Master curves for storage modulus for polycyanurate networks with different cross-link densities; the molar monofunctional monomer concentration x_M and the reference temperature for each curve are indicated.

moduli functions suggests the validity of the time−temperature superposition principle.

The effect of cross-link density on the viscoelastic response of this polycyanurate is examined by changing the concentration of monofunctional monomer in the formulation. The resulting master curves for the storage, loss, and relaxation moduli are compared in Figures 5−7. The reference temperature for each formulation is the nominal glass transition temperature (i.e., T_f') obtained from DSC. At low frequencies or long times, the materials show a rubbery response; the rubbery modulus increases with decreasing monofunctional monomer concentration (i.e., with increasing cross-link density) and depends on temperature. At high frequencies or short times, glassy behavior is observed, and the glassy modulus G_g is found to be independent of temperature and monofunctional monomer concentration (i.e., cross-link density). The glassy and rubbery moduli for the polycyanurate networks are listed in Table 2.

The reduced curves for G' and G'' were fit to eqs 1 and 2 using the Innovative Rheological Interface Software (IRIS, version 8.0) developed by Winter and co-workers at the University of Massachusetts Amherst.[60] From the fitting procedure, the discrete relaxation spectra, g_i as a function of τ_i, are determined and will be discussed later. The model curves

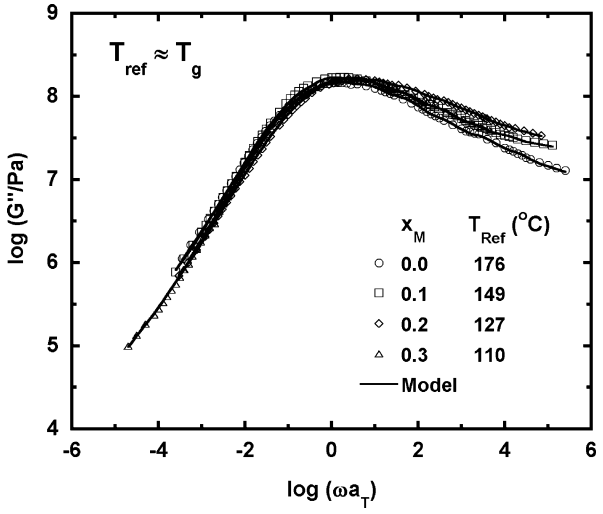

Figure 6. Master curves for loss modulus for polycyanurate networks with different cross-link densities; the molar monofunctional monomer concentration x_M and the reference temperature for each curve are indicated.

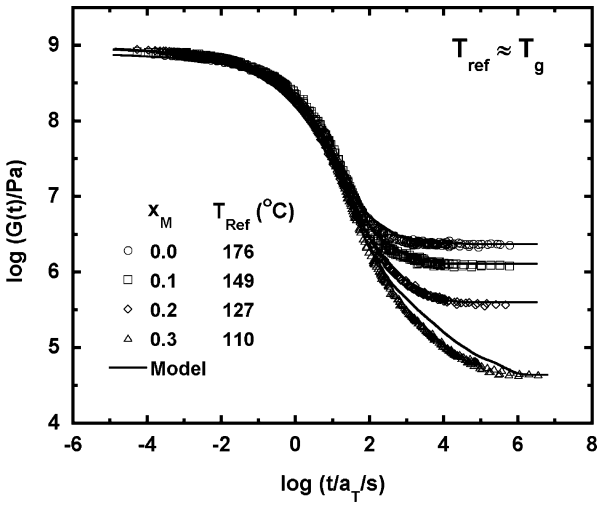

Figure 7. Master curves for relaxation modulus for polycyanurate networks with different cross-link densities; the molar monofunctional monomer concentration x_M and the reference temperature for each curve are indicated.

Table 2. Glassy and Rubbery Moduli of Polycyanurate Networks as a Function of Monofunctional Monomer Concentration

x_M (mole fraction)	G_g (MPa)[a]	G_r (MPa)[a,b]
0.0	797 ± 4	0.0050T ± 0.04
0.1	842 ± 18	0.0028T ± 0.025
0.2	842 ± 25	0.00089T ± 0.013
0.3	765 ± 9	0.00011T ± 0.001

[a] The data include the standard deviation for G_g and G_r. The standard deviation for G_g was calculated from the scatter in the limiting high-frequency value obtained from dynamic measurements, whereas the standard deviation for the G_r was determined from the scatter in the limiting long-time value obtained from stress relaxation measurements. [b] The temperature T in the equation for G_r is in kelvin.

are shown as solid lines in Figures 5−7, and they describe the data well. Note that the model for the relaxation modulus (Figure 7) is a prediction based on the fits of the dynamic data since fitting relaxation data to eq 3 is an ill-posed problem.[61]

The shift factors used to reduce the viscoelastic data in Figures 5−7 are plotted in Figure 8 against the temperature departure from T_g (i.e., against $T - T_g$, where T_g differs for each formulation, as indicated in the legends of Figures 5−7). The

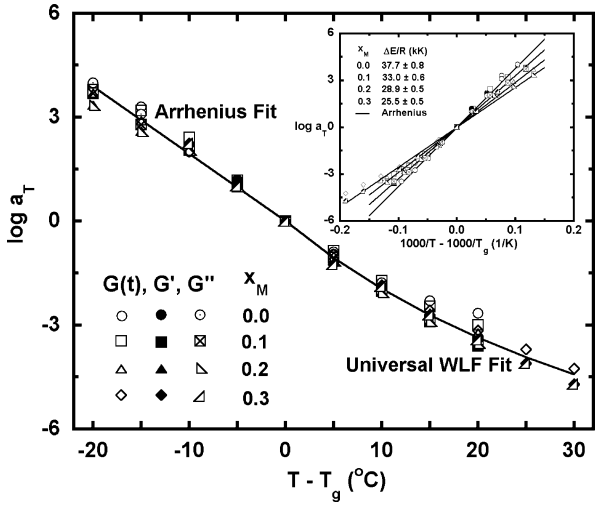

Figure 8. Shift factors as a function of the temperature departure from T_g ($T - T_g$) for polycyanurate networks. The inset plots the shift factors against the relative reciprocal temperature ($1/T - 1/T_g$). The molar monofunctional monomer concentration x_M is indicated. The symbols for $G(t)$, G', and G'' in the inset are the same as those in the main figure.

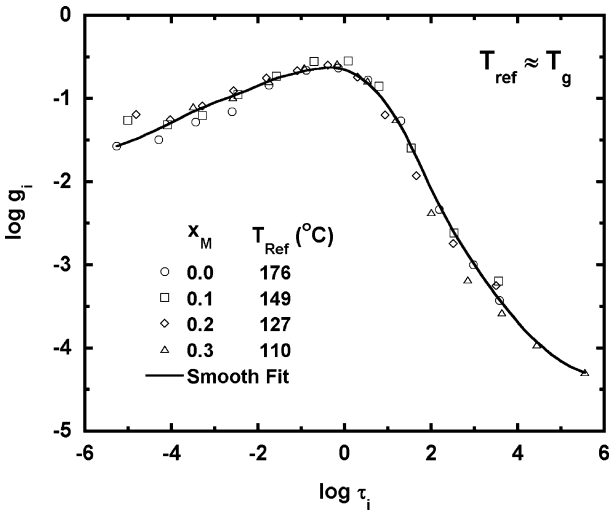

Figure 9. Discrete relaxation spectra for polycyanurate networks with different cross-link densities; the molar monofunctional monomer concentration x_M and the reference temperature for each data set are indicated.

shift factors for $G(t)$, G', and G'' agree well with one another for each formulation, indicating that the data are consistent. The temperature dependences of the shift factors for the various formulations are also similar and follow the Arrhenius equation below their respective T_gs and the "universal" WLF equation[48] above T_g. When the shift factors are plotted as a function of relative reciprocal temperature, $1/T - 1/T_g$, they show an Arrhenius temperature dependence due to the limited temperature range of the measurements, as indicated in the inset. The resulting apparent activation energy increases with decreasing monofunctional monomer concentration (i.e., with increasing cross-link density) since T_g is a function of cross-link density; the apparent activation energies are tabulated in the inset. However, given that the shift factors show the same dependence on $T - T_g$, the temperature−cross-link density superposition principle[39−43,49−52] is expected to be valid for this series of polycyanurate networks.

As mentioned earlier, the discrete relaxation spectra $g_i(\tau_i)$ were generated by fitting the dynamic data to eqs 1 and 2; the double-logarithmic g_i vs τ_i is plotted in Figure 9. The discrete

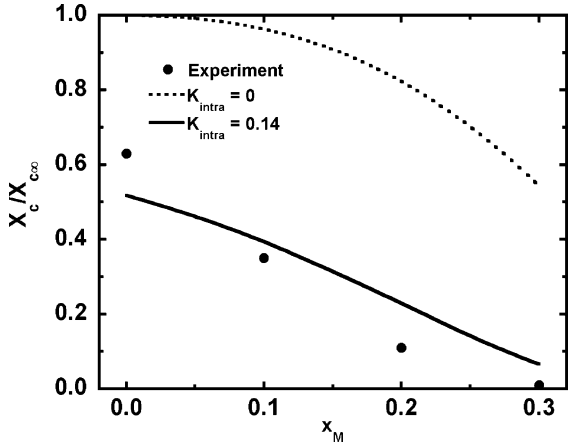

Figure 10. Relative cross-link density for polycyanurate networks vs mole fraction of monofunctional monomer.

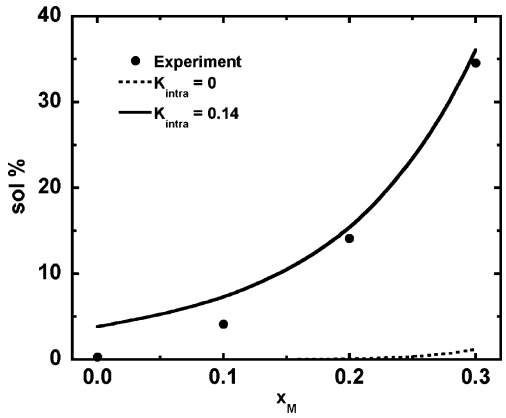

Figure 11. Sol content for polycyanurate networks vs mole fraction of monofunctional monomer.

relaxation spectra $g_i(\tau_i)$ are independent of monofunctional monomer concentration (i.e., cross-link density) within the relaxation time window investigated, corroborating the validity of time−cross-link density superposition. In contrast, the relaxation spectra $H(\tau)$ and the retardation spectra $L(\lambda)$ of rubber and epoxy networks studied in other works[40,41,50,51] are found to be independent of cross-link density at short times, but the width of the spectra broadens with decreasing cross-link density at long times in both rubber and epoxy networks. However, the reader is reminded that in these references,[40,41,50,51] where the retardation or relaxation spectra depended on cross-link density at long times, time−cross-link density superposition was still found to be experimentally valid in the dispersion region. We note that the modulus (or relaxation time spectrum) better reveals short-time processes and the compliance (or retardation time spectrum) better reveals long-time processes;[44] hence, one possibility for why we do not see a change in our spectra with cross-link density at long times may be that we measured the modulus. On the other hand, other researchers[51] measured the modulus in vulcanized butadiene styrene rubbers (SBR) and saw changes in the breadth of the spectrum with cross-link density. Perhaps a better reason for our spectra's lack of dependence on cross-link density is that although a portion of the triazine rings are not elastically effective in the formulations with monofunctional monomer, these rings may contribute to the stiffness of the network and influence the long time mechanisms, as has been proposed by other researchers.[38,58] Hence, the independence of our relaxation spectra on the cross-link density in the long time region may in part be due to the unique nature of the polycyanurate network structure in which a branch point is

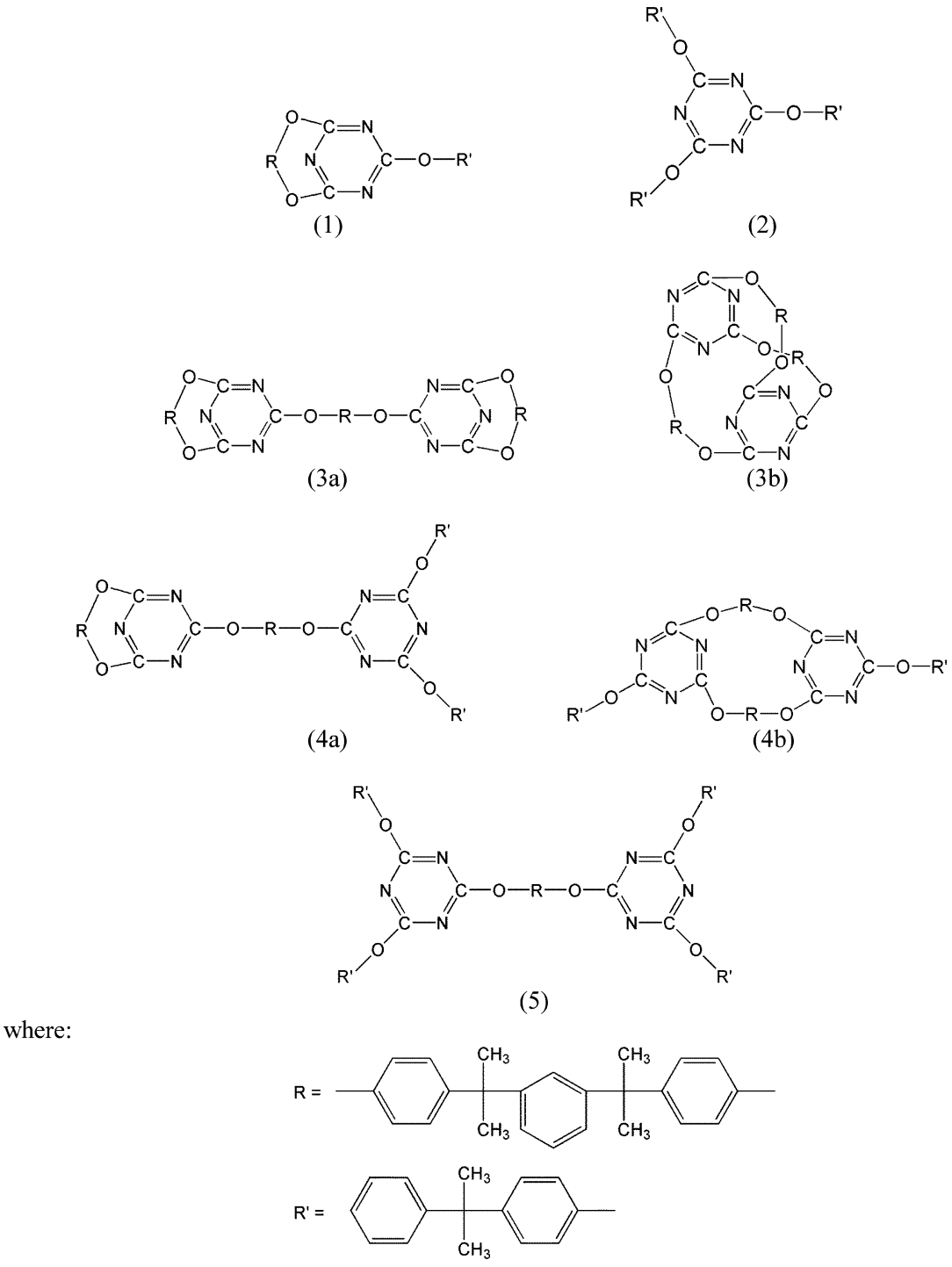

Figure 12. Schematic structures for the two principal species (**1**) and (**2**) and three minor species (**3a,b**), (**4a,b**), and (**5**) in the sol extracted from the polycyanurate network containing 0.3 mole fraction of monofunctional monomer.

produced every time a functional group trimerizes (except for the functional groups that react intramolecularly prior to gelation).

Cross-Link Density and Sol Content of Polycyanurate Networks. The experimental cross-link density, X_c (or the concentration of the junction points in the infinite network,[57] in molar number of the junction points per volume), can be determined from the viscoelastic data based on the theory of rubber elasticity:[45,57]

$$G_r = \nu RT = \frac{1}{2} X_c RT \qquad (5)$$

where G_r is the measured rubbery modulus, ν is the effective concentration of network chains which is assumed to equal the concentration of chemical cross-links, R is the gas constant, and T is absolute temperature. The prefactor $^1/_2$ accounts for the number of weighted network chains attached to each cross-link.[57] The relative cross-link density, $X_c/X_{c\infty}$, for the polycyanurate networks with different monofunctional cyanate ester concentrations is plotted in Figure 10. $X_{c\infty}$, which equals $[D]_0/3$, is the cross-link density of the neat ideal polycyanurate network formed from difunctional monomer in the absence of intracyclization reactions, where $[D]_0$ is the initial concentration of cyanate ester functional groups in the neat resin (5.76 mol/

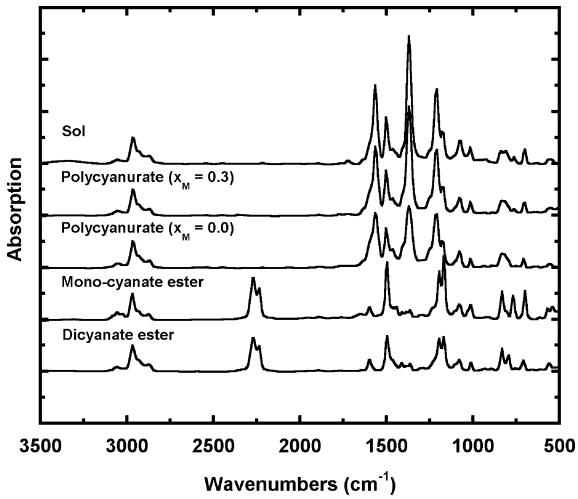

Figure 13. FTIR spectra for (from bottom to top) the difunctional monomer, the monofunctional monomer, the polycyanurate without monofunctional monomer, the polycyanurate with 0.3 mole fraction of monofunctional cyanate ester, and the sol extracted from the polycyanurate having 0.3 mole fraction of monofunctional cyanate ester. Curves are offset for clarity.

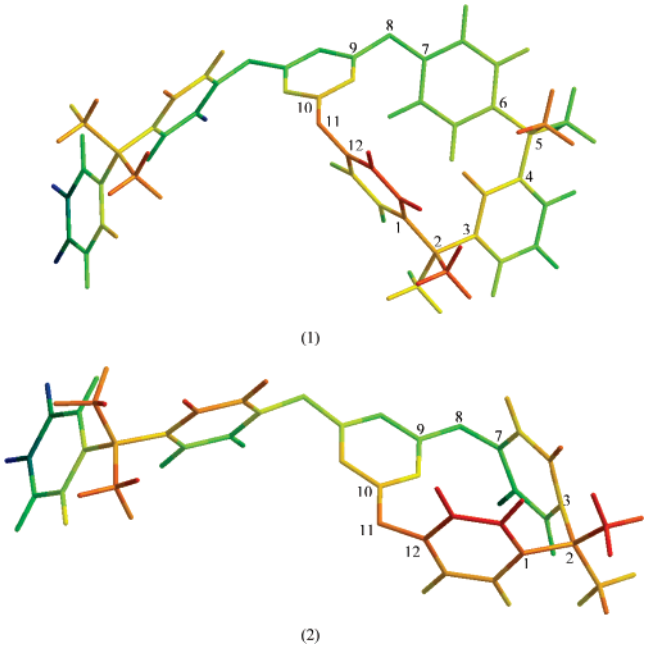

Figure 14. 3-D models for the dimers from (**1**) one bisphenol M dicyanate ester and one monofunctional cyanate ester and (**2**) one bisphenol A dicyanate ester and one monofunctional cyanate ester, as generated by Chem3D Pro 8.0.

dm^3) and the prefactor $^1/_3$ is incorporated because each effective cross-link point is formed by three cyanate ester groups under ideal conditions. The relative cross-link density at full conversion decreases with increasing monofunctional monomer concentration. In addition, it is important to note that the formulation having no monofunctional monomer ($x_M = 0$) has a considerably lower cross-link density than would be expected in the absence of intracyclization reactions (i.e., $X_c/X_{c\infty}$ is significantly less than 1.0). Also shown in Figure 10 are calculations of the relative cross-link density based on the recursive method. The dashed line represents the theoretical result obtained assuming no intracyclization prior to gelation, which predicts cross-link densities significantly higher than the experimental values. However, when monomer cyclization is taken into account, the theoretical calculation with $K_{intra} = 0.14$ describes the experimental data well.

Sol extraction results are shown in Figure 11. The sol content is found to increase with increasing monofunctional monomer concentration. The theoretical calculation assuming no monomer cyclization significantly underestimates the sol content. On the other hand, the experimental sol content is well described by the recursive calculation modified to include monomer cyclization, with $K_{intra} = 0.14$.

The occurrence of monomer cyclization is confirmed by the results obtained from mass spectroscopy. The chemical composition of the sol extracted from the formulation with 0.3 mole fraction of monofunctional cyanate ester was identified upon mass spectroscopy analysis. Two major peaks at 634 and 712 *m*/*z* and three minor peaks at 1189, 1267, and 1345 *m*/*z* appeared on the spectra. Analysis of these peaks suggests that the sol is comprised of two principal species whose structures are shown in Figure 12: (**1**) the dimer formed by trimerization of three functional groups, one from a monofunctional monomer and two from the same difunctional monomer (63.7%), and (**2**) the trimer of monofunctional cyanate ester (35.4%). The concentration of the species in the sol is noted parenthetically in the previous sentence and was determined by assuming that all species have the same ability of being ionized. In addition to the two principal species, three minor species, whose structures are also shown in Figure 12, are also present: (**3**) the trimer of difunctional cyanate ester (0.2%), (**4**) the tetramer of two difunctional and two monofunctional cyanate esters (0.4%), and (**5**) a pentamer from one difunctional and four monofunctional cyanate esters (0.3%). Note that structures **3** and **4** could either arise from monomer cyclization (as drawn in **3a** and **4a**) or could arise from participation of the ends of two difunctional monomers in the same two triazine rings (structures **3b** and **4b**). Structure **3b**, in fact, was proposed by Fang et al.[27,28] on the basis of mass spectroscopy of the reaction products of BADC; a similar structure was proposed by Wang and Hong,[18] who studied partially cured DSCI by mass spectroscopy. However, the presence of dimer, structure **1** in Figure 12, confirms monomer cyclization and leads us to speculate that structures **3a** and **4a** may be more probable than **3b** and **4b** in some dicyanate esters. The presence of the dimer as a major component in the sol in this formulation is also corroborated by the fact that the glass transition temperature of the sol is 35 °C, around 5 K lower than that for the trimer of monofunctional cyanate ester cured isothermally at 180 °C for 18 h, indicating that the sol includes species of lower molecular weight than the trimer of monofunctional monomer—note that the dimer molecular weight is 633 g/mol, whereas the trimer of monofunctional monomer is 711 g/mol.

Results from FTIR analysis of the sol, the monomers, and the polycyanurate network with and without monofunctional cyanate ester are also consistent with those from mass spectroscopy. Representative FTIR spectra, shown in Figure 13, indicate that the sol comprises oligomers from the trimerization reactions of monofunctional and/or difunctional cyanate esters with no unreacted cyanate ester functional groups present; note the presence of the triazine and polycyanurate absorption peaks at 1373 and 1565 cm^{-1} in the sol and the lack of the strong peaks associated with the cyanate group at 2237 and 2276 cm^{-1}. Similarly, the fully cured polycyanurates show no indication of unreacted functional groups.

The existence of the dimer from one monofunctional and one difunctional cyanate ester as a result of monomer cyclization (structure **1** in Figure 12) is further supported by the modeling of 3-D molecular structures of the BMDC dimer using Chem3D Pro 8.0. Similar modeling is also performed on bisphenol A

Table 3. Bond Angle (deg) and Bond Length (Å) on the Intramolecular Loop and Triazine Ring of the Dimer from One Difunctional and One Monofunctional Cyanate Ester

	dimer from bisphenol M dicyanate and monofunctional monomer		dimer from bisphenol A dicyanate and monofunctional monomer		literature values	
linkages	bond angle	av bond length	bond angle	av bond length	bond angle	av bond length
C1−C2−C3	105.3	1.578	95.3	1.559	109.5	1.54
C4−C5−C6	115.3		N/A		109.5	
C7−O8−C9	106.5	1.431	107.9	1.421	112.0	1.43
C10−O11−C12	106.9		115.8		112.0	
C−N−C	118.9	1.327	120.0	1.336	112.6	1.324
N−C−N	121.5		120.3		127.4	

dicyanate ester (BADC) and its dimer with one monofunctional monomer. The 3-D models for the two dimers are shown in Figure 14. The bond angle and bond lengths in the monomeric loop and triazine ring of the dimers are compared with the crystallographic data in the literature[62,63] and are tabulated in Table 3. All of the bond angles are within ±6° of the literature values for the dimer of the BMDC monomer, and the bond lengths are within 0.05 Å. Similar results are found for the dimer of the BADC monomer, except that the C−C−C linkage on the intramolecular loop of the dimer from bisphenol A dicyanate ester and monofunctional monomer (C1−C2−C3 in Figure 14 (**2**)) sustains more constraint with a bond angle 14° smaller than the literature value, and the bonds in the triazine ring show strains of ±7° from the literature; all of the bond lengths are comparable with the literature values. The successful modeling of the dimer structures suggests that these species do exist within the normal energy scale. Furthermore, the formation of monomeric loops via monomer cyclization is suggested to be an important cause of the decreased effective cross-link density and increased sol content relative to the values expected in the absence of intracyclization which we observe in this study.

Discussion

Any reactivity difference of cyanate groups on the monofunctional and difunctional cyanate esters will influence the cross-link density and sol content.[23] The triazine rings formed in the system with both monofunctional and difunctional monomers may be effective cross-link points, branch points, part of dangling chains, or part of small molecules. When the cyanate groups on the two monomers have equal reactivities, the amount of these four species only depends on the conversion and the initial molar ratio of the two monomers. However, if the reactivities of cyanate groups on the two monomers differ significantly, the resulting network would be comprised primarily of the reacted difunctional monomer, whereas the sol would be comprised primarily of the trimer of the monofunctional monomer. Consequently, both the cross-link density and the sol content would be expected to be greater than for networks formed by two monomers with equal reactivity. The higher cross-link density expected assuming unequal reactivity contradicts our experimental results, suggesting that it is not the unequal reactivity but monomer cyclization that leads to the large discrepancy in cross-link density and sol content between experiment and theory. The comparable reactivity of the monofunctional and difunctional monomers assumed in the present work is also validated by the literature data. Bauer et al. showed that 4tbutPC, a monofunctional monomer with a similar structure as the one used in the current study (except that 4tbutPC has a methyl group terminated chain end rather than a phenyl group), and BMDC, the difunctional monomer used in this study, have similar reactivity using various techniques.[23]

Intracyclization has been proposed by many researchers as a significant factor contributing to the gelation delay of dicyanate esters.[12,15,18,27,28,31,64] To date, all of the intracyclization referred to in the literature involve two cyanate groups on the same *oligomer* reacting with a third functional group resulting in macrocyclic ring formation.[12,31] However, the analysis of chemical composition of the extracted sol in the current study suggests that intracyclization involving two cyanate groups on the same difunctional *monomer* reacting with a third cyanate group from another monomer, or monomer cyclization, occurs during the cure of bisphenol M dicyanate and monofunctional monomer. For the cyanate esters with similar structures as bisphenol M and bisphenol A dicyanate esters, monomer cyclization may also occur during their curing reactions. The 3-D molecular structures of the dimers from the various difunctional cyanate esters listed in Table 1 and the monofunctional monomer were modeled using Chem 3D Pro 8.0 software. Except for one case, all of the dimers from the other dicyanate esters and the monofunctional monomer were successfully modeled. A weak inverse correlation between the bond strains in the triazine ring and the conversion at gelation was observed: monomers with the lowest bond strains in the triazine ring (BMDC and TMBADC, with bond angles within ±6° of literature values) show gelation at greater than 60% conversion, whereas monomers with the highest degree of bond strains in the triazine ring show conversions at gelation nearer to the ideal value (such as HFBADC and F_6CY which show bond strains in the triazine ring of 10° and 9°, respectively). The monomer TDPC, however, showed the greatest degree of triazine ring strain and its C−S center bond is lengthened by 0.3 Å, and yet, this monomer gels at a conversion of 0.58; in this case, the delayed gelation behavior must be attributed to oligomer cyclization rather than monomer cyclization. Similarly for the monomer DCSI, the dimer of DCSI and the monofunctional monomer could not be modeled, and consequently, the delayed gelation of DCSI must be attributed to the oligomer cyclization. In addition, it is important to note that the probability of monomer cyclization for monomers with long and flexible backbones, such as F_6CY and CPS, decreases as the backbone length increases due to an increasing ability to examine space,[65] and as a result, the gelation of these two monomers is less delayed. It is suggested that for bisphenol M and bisphenol A dicyanate esters and other cyanate esters with similar chemical structure such as bis(4-cyanatophenyl) ether (OXOCY),[19] dicyanato-4,4′-diphenylethane (DPEDC),[16,17] and tetramethylbisphenol-A dicyanate (TMBADC),[12] monomer cyclization may be more likely to occur and is an important contributor to the gelation delay. Hence, although considering monomer cyclization as the only intramolecular cyclization reaction that occurs before gelation is an oversimplification, for some systems, such as the BMDC studied here, this approach explains the network structure and delayed gelation in a consistent way.

Conclusions

The shear viscoelastic response of bisphenol M dicyanate ester/polycyanurate networks is presented as a function of cross-

link density, varied by changing the ratio of difunctional to monofunctional cyanate ester monomers in the formulations. Both stress relaxation and dynamic experimental data are shown. Master curves are constructed following the time−temperature superposition principle, and the temperature dependence of the shift factors is independent of cross-link density when plotted as a function of $T - T_g$; however, since T_g is a function of cross-link density, the apparent activation energy increases with increasing cross-link density. The shear response can be described by the sum of Maxwell elements, and the discrete relaxation spectra are found to be independent of the cross-link density. The rubbery modulus decreases with decreasing cross-link density, but the decrease is larger than expected on the basis of theoretical calculations assuming equal reactivity and no intracyclization. The discrepancy indicates that the assumptions underlying the recursive calculation are invalid for this thermosetting system. Rather, for these materials, we find on the basis of mass spectroscopy of the sol that a monomer cyclization reaction occurs, leading to loop formation and increased sol content. With the incorporation of the monomer cyclization, good agreement was obtained between the theory and experiment for both the cross-link density and the sol content. The probability of monomer cyclization was determined to be 0.14; this value predicts that the conversion at gelation should be 0.63 for neat bisphenol M dicyanate ester, consistent with the experimental value of 0.64, and suggesting that monomer cyclization is able to explain the network structure and delayed gelation in a consistent way for the bisphenol M dicyanate ester systems studied. The monomer cyclization reaction may also be an important factor for bisphenol A dicyanate ester and other monomers with similar structure.

Acknowledgment. Funding from NSF-DMR 0308762 is gratefully acknowledged. The authors also thank Dr. V. Krishnamachari and Professor P. Pare in the Department of Chemistry and Biochemistry at Texas Tech University for their help with mass spectroscopy analysis. Help and valuable discussions from Dr. X. Shi, Mr. S. A. Hutcheson, and Professor G. B. McKenna in the Department of Chemical Engineering at Texas Tech University are also greatly acknowledged.

Appendix. Application of Recursive Theory to the Calculation of Network Parameters of Dicyanate Ester/Polycyanurate Systems

The properties of dicyanate ester/polycyanurate systems before and after the gelation, such as the gel point, cross-link density, and sol content, can be computed using the recursive theory developed by Miller and Macosco.[57] Generally, assumptions of no intracyclization reactions before gelation and equal reactivity are made, but here we incorporate a monomer cyclization reaction in which the two functional groups from the same difunctional monomer react with a third functional group from another monomer. We assume that the probability of two cyanate groups on the same monomer reacting with each other is K_{intra}. Then, for the system with neat difunctional cyanate ester, following the notation of Miller and Macosco,[57] the probability of finding a finite chain when looking out from a randomly chosen cyanate ester group D, $P(F_D^{out})$, is

$$\begin{aligned} P(F_D^{out}) = {} & P(F_D^{out}|D_{\text{does not react}}) + \\ & P(F_D^{out}|D_{\text{reacts with one D from its own and one D from another}}) + \\ & P(F_D^{out}|D_{\text{reacts with two Ds from the same different monomer}}) + \\ & P(F_D^{out}|D_{\text{reacts with two Ds from two different monomers}}) \\ = {} & (1-\beta_D)(1) + \beta_D[K_{intra}P(F_D^{in}) + K_{intra} + \\ & (1-2K_{intra})(P(F_D^{in}))^2] \end{aligned} \quad \text{(A1)}$$

where β_D be the conversion. Since $P(F_D^{out}) = P(F_D^{in})$, $P(F_D^{out})$ can be obtained by solving eq A1:

$$P(F_D^{out}) = \frac{1-\beta_D K_{intra}}{\beta_D - 2\beta_D K_{intra}} - 1 \quad \text{(A2)}$$

The relative cross-link density ($X_c/X_{c\infty}$) and the sol content (w_s) are related to $P(F_D^{out})$:

$$\frac{X_c}{X_{c\infty}} = \beta_D(1 - P(F_D^{out}))^3 \quad \text{(A3)}$$

$$w_s = (P(F_D^{out}))^2 \quad \text{(A4)}$$

where $X_{c\infty}$ is the cross-link density of the polycyanurate network from neat dicyanate ester with a perfect network structure, i.e., with no intracyclization reaction, which equals $[D]_0/3$. Note that eq A3 contains a leading conversion term similar to the work of Lin et al.[12,31,38,58] but differing from the original derivation of Simon and Gillham:[1] the reason for this is that the probability of any randomly chosen functional group being a cross-link point is zero if the functional group is unreacted, whereas the probability is equal to the probability of finding three infinite arms if the group is reacted, thus yielding the expression shown in eq A3. The conversion at the point of gelation, β_{gel}, can be obtained from eq A2 following the approach of Miller and Macosko:[57]

$$\beta_{gel} = \frac{1}{2 - 3K_{intra}} \quad \text{(A5)}$$

Given that the delayed gel point measured experimentally for BMDC is 0.64, K_{intra} should be 0.146 assuming that the only intramolecular cyclization reaction that occurs before gelation is monomer cyclization.

The recursive method is also applicable to the cyanate ester/polycyanurate networks which contain monofunctional and difunctional monomer. For such systems, the probability of finding a finite chain when looking out from a randomly chosen functional group on the monofunctional monomer M, $P(F_M^{out})$, is given by

$$\begin{aligned} P(F_M^{out}) = {} & P(F_M^{out}|M_{\text{does not react}}) + P(F_M^{out}|M_{\text{reacts with two Ms}}) + \\ & P(F_M^{out}|M_{\text{reacts with one M and one D}}) + \\ & P(F_M^{out}|M_{\text{reacts with two Ds from the same monomer}}) + \\ & P(F_M^{out}|M_{\text{reacts with two Ds from two different monomers}}) \\ = {} & (1-\beta_M)(1) + \beta_M[x_M{}^2 + 2x_M x_D P(F_D^{in}) + \\ & K_{intra}x_D{}^2 + (1-K_{intra})x_D{}^2(P(F_D^{in}))^2] \end{aligned} \quad \text{(A6)}$$

where β_M is the conversion of M, and x_M and x_D are the mole fractions of cyanate groups that belong to monofunctional and difunctional monomers, respectively. Similarly, the probability of finding a finite chain when looking out from a randomly chosen functional group on the difunctional monomer D, $P(F_D^{out})$, is given by

$$P(F_D^{out}) = P(F_D^{out}|D_{\text{does not react}}) + P(F_D^{out}|D_{\text{reacts with two Ms}}) + P(F_D^{out}|D_{\text{reacts with one M and one D from its own}}) + P(F_D^{out}|D_{\text{reacts with one M and one D from another monomer}}) + P(F_D^{out}|D_{\text{reacts with two Ds, one from its own and one from another monomer}}) + P(F_D^{out}|D_{\text{reacts with two Ds from the same different monomer}}) + P(F_D^{out}|D_{\text{reacts with two Ds from two different monomers}})$$

$$= (1 - \beta_D)(1) + \beta_D[x_M^2 + K_{intra}x_Mx_D + (2 - K_{intra})x_Mx_DP(F_D^{in})] + \beta_D[K_{intra}x_D^2P(F_D^{in}) + K_{intra}x_D^2 + (1 - 2K_{intra})x_D^2(P(F_D^{in}))^2] \quad \text{(A7)}$$

Since $P(F_D^{in}) = P(F_D^{out})$, $P(F_D^{out})$ can be calculated by solving eq A7, which in turn yields $P(F_M^{out})$. The relative cross-link density and the sol content are related to $P(F_D^{out})$ and $P(F_M^{out})$:

$$\frac{X_c}{X_{c\infty}} = w_D\beta_D(1 - P(F_D^{out}))^3 \quad \text{(A8)}$$

$$w_s = w_M(P(F_M^{out})) + w_D(P(F_D^{out}))^2 \quad \text{(A9)}$$

where w_M and w_D are the weight fractions of monofunctional and difunctional cyanate esters, respectively. The conversion at the point of gelation can also be calculated following the approach of Miller and Macosco:[57]

$$\beta_{gel} = \frac{1}{2x_D[1 - K_{intra}(x_D + 1/2)]} \quad \text{(A10)}$$

References and Notes

(1) Simon, S. L.; Gillham, J. K. *J. Appl. Polym. Sci.* **1993**, *47*, 461.
(2) Bauer, M.; Bauer, J. *Makromol. Chem., Macromol. Symp.* **1989**, *30*, 1.
(3) Bauer, M.; Bauer, J. *Makromol. Chem., Macromol. Symp.* **1993**, *76*, 201.
(4) Georjon, O.; Galy, J.; Pascault, J.-P. *J. Appl. Polym. Sci.* **1993**, *49*, 1441.
(5) Kasehagen, L. J.; Macosko, C. W. *Polym. Int.* **1997**, *44*, 237.
(6) Stutz, H.; Simak, P. *Macromol. Chem.* **1993**, *194*, 3031.
(7) Mormann, W.; Zimmerman, J. *Makromol. Symp.* **1995**, *93*, 97.
(8) Gupta, A. N.; Macosko, C. W. *Macromolecules* **1993**, *26*, 2455.
(9) Osei-Owusu, A.; Martin, G. C.; Gotro, J. T. *Polym. Eng. Sci.* **1991**, *31*, 1604.
(10) Grenier-Loustalot, M.; Lartigau, C.; Grenier, J. *J. Polym. Sci., Part A: Polym. Chem.* **1996**, *34*, 2955.
(11) Deng, Y.; Martin, G. C. *J. Appl. Polym. Sci.* **1997**, *64*, 115.
(12) Lin, R. H.; Su, A. C.; Hong, J. L. *J. Appl. Polym. Sci.* **1999**, *73*, 1927.
(13) Shimp, D. A.; Christenson, J. R.; Ising, S. J. In 3rd Int. SAMPE Elec. Mater. Proc., Los Angeles, CA, 1989.
(14) Recalde, I. B.; Campos, A.; Gomez, C. M.; Mondragon, I.; Harismendy, I. *Int. J. Polym. Anal. Charact.* **2001**, *6*, 481.
(15) Korshak, V. V.; Pankratov, V. A.; Ladovskaya, A. A.; Vinogradova, A. V. *J. Polym. Sci.: Polym. Chem.* **1978**, *16*, 1697.
(16) Galy, J.; Gerard, J. F.; Pascault, J. P. In *Polyimides and High Temperature Polymerization*; Proceedings of the European Technical Symposium; Abadie, M. J. M., Sillion, B., Eds.; Elsevier: Amsterdam, 1991.
(17) Chen, Y.-T.; Macosko, C. W. *J. Appl. Polym. Sci.* **1996**, *62*, 567.
(18) Wang, F. L.; Hong, J. L. *Polymer* **1998**, *39*, 4319.
(19) Armistead, J. P.; Snow, A. W. *ACS Div. Polym. Mater. Sci. Eng.* **1992**, *66*, 437.
(20) Snow, A. W.; Buckley, L. J.; Armistead, J. P. *J. Polym. Sci., Part A: Polym. Chem.* **1999**, *37*, 135.
(21) Lu, M.-C.; Hong, J.-L. *Polymer* **1994**, *35*, 2822.
(22) Pankratov, V. A.; Vinogradova, S. V.; Korshak, V. V. *Russ. Chem. Rev.* **1977**, *46*, 278.
(23) Bauer, J.; Hoper, L.; Bauer, M. *Macromol. Chem. Phys.* **1998**, *199*, 2417.
(24) Bauer, M.; Bauer, J. Chemistry and Technology of Cyanate Ester Resins. In *Aspects of the Kinetics, Modeling and Simulation of Network Build-up during Cyanate Ester Cure*; Hamerton, I., Ed.; Blackie Academic & Professional: London, 1994.
(25) Cozzens, R.; Walter, P.; Snow, A. W. *J. Appl. Polym. Sci.* **1987**, *34*, 601.
(26) Deng, Y.; Martin, G. C. *Polymer* **1996**, *37*, 3593.
(27) Fang, T.; Houlihan, F. M. *ACS Polym. Prepr.* **1994**, *35*, 535.
(28) Fang, T.; Shimp, D. A. *Prog. Polym. Sci.* **1995**, *20*, 61.
(29) Fyfe, C. A.; Niu, J.; Rettig, S. J.; Burlinson, N. E.; Reisema, C. M.; Wang, D. W.; Poliks, M. *Macromolecules* **1992**, *25*, 6289.
(30) Lin, K.; Shyu, J. *J. Polym. Sci., Part A: Polym. Chem.* **2001**, *39*, 3085.
(31) Lin, R. H.; Hong, J. L.; Su, A. C. *Comput. Theor. Polym. Sci.* **1997**, *7*, 95.
(32) Osei-Owusu, A.; Martin, G. C.; Gotro, J. T. *Polym. Eng. Sci.* **1992**, *32*, 535.
(33) Papathomas, K. I.; Wang, D. W. *J. Appl. Polym. Sci.* **1992**, *44*, 1267.
(34) Reghunadhan, Nair, C. P.; Mathew, D.; Ninan, K. N. *Adv. Polym. Sci.* **2001**, *155*, 1.
(35) Flory, P. J. *J. Am. Chem. Soc.* **1941**, *63*, 3083.
(36) Deng, T. H.; Knauss, W. G. *Mech. Time-Depend. Mater.* **1997**, *1*, 33.
(37) Davies, J. M. R.; Hamerton, I.; Jones, J. R.; Povey, D. C.; Barton, J. M. *J. Crystallogr. Spectrosc. Res.* **1990**, *20*, 287.
(38) Lin, R. H.; Su, A. C.; Hong, J. L. *J. Polym. Sci., Part B: Polym. Phys.* **2000**, *38*, 726.
(39) Lee, A.; McKenna, G. B. *Polymer* **1988**, *29*, 1812.
(40) Plazek, D. J.; Choy, I.-C. *J. Polym. Sci., Part B: Polym. Phys.* **1989**, *27*, 307.
(41) Plazek, D. J.; Chay, I.-C. *J. Polym. Sci., Part B: Polym. Phys.* **1991**, *29*, 17.
(42) Simon, S. L.; McKenna, G. B.; Sindt, O. *J. Appl. Polym. Sci.* **2000**, *76*, 495.
(43) Suzuki, K.; Miyano, Y. *J. Appl. Polym. Sci.* **1977**, *21*, 3367.
(44) Ferry, J. D. *Viscoelastic Properties of Polymers*; John Wiley & Sons: New York, 1980.
(45) Treloar, L. R. G. *The Physics of Rubber Elasticity*, 3rd ed.; Clarendon Press: Oxford, 1975.
(46) Vogel, H. *Phys. Z.* **1921**, *22*, 645.
(47) Fulcher, G. S. *J. Am. Chem. Soc.* **1925**, *8*, 339.
(48) Williams, M. L.; Landell, R. F.; Ferry, J. D. *J. Am. Chem. Soc.* **1955**, *77*, 3701.
(49) Plazek, D. J. *J. Polym. Sci., Part A2* **1966**, *4*, 745.
(50) Valentine, R.; Ferry, J. D.; Homma, T.; Ninomiya, K. *J. Polym. Sci., Part A2: Polym. Phys.* **1968**, *6*, 479.
(51) Thirion, P.; Chasset, R. *Pure Appl. Chem.* **1970**, *23*, 183.
(52) Arenz, R. J. *J. Polym. Sci., Part B: Polym. Phys.* **1974**, *12*, 131.
(53) Moynihan, C. T.; Easteal, A. J.; DeBolt, M. A.; Tucker, J. *J. Am. Ceram. Soc.* **1976**, *59*, 12.
(54) Badrinarayanan, P.; Zheng, W.; Li, Q.; Simon, S. L. *J. Non-Cryst. Solids*, submitted for publication.
(55) Struik, L. C. E. *Physical Aging in Amorphous Polymers and Other Materials*; Elsevier Scientific: Amsterdam, 1978.
(56) Schröter, K.; Hutcheson, S. A.; Shi, X.; Mandanici, A.; McKenna, G. B. *J. Chem. Phys.* **2006**, *125*, 214507.
(57) Miller, D. R.; Macosko, C. W. *Macromolecules* **1976**, *9*, 206.
(58) Lin, R. H.; Su, A. C.; Hong, J. L. *Polym. Int.* **2000**, *49*, 345.
(59) Sarmoria, C.; Miller, D. R. *Comput. Theor. Polym. Sci.* **2001**, *11*, 113.
(60) http://rheology.tripod.com/, In.
(61) Mours, M.; Winter, H. H. *IRIS Handbook, the IRIS Method of Merging Experiment with Theory in Rheology*; IRIS Development LLC: Amherst, MA, 2004.
(62) Allington, R. D.; Attwood, D.; Hamerton, I.; Hay, J. N.; Howlin, B. J. *Comput. Theor. Polym. Sci.* **2001**, *11*, 467.
(63) Allington, R. D.; Attwood, D.; Hamerton, I.; Hay, J. N.; Howlin, B. J. *Polymer* **2003**, *44*, 793.
(64) Lin, R. H.; Su, A. C.; Hong, J. L. *J. Polym. Sci., Part B: Polym. Phys.* **2000**, *38*, 726.
(65) Flory, P. J. *Principles of Polymer Chemistry*; Cornell University Press: Ithaca, NY, 1953.

MA0624144